





Article

Effects of Structural Radiation Disorder in the Near-Surface Layer of Alloys Based on NbTiVZr Compounds Depending on the Variation of Alloy Components

Sholpan G. Giniyatova ¹, Kayrat K. Kadyrzhanov ^{1,*}, Dmitriy I. Shlimas ^{1,2}, Daryn B. Borgekov ^{1,2}, Vladimir V. Uglov ³, Artem L. Kozlovskiy ^{1,4} and Maxim V. Zdorovets ^{1,2}

¹ Engineering Profile Laboratory, L.N. Gumilyov Eurasian National University, Satpayev St., Astana 010008, Kazakhstan; mzdorovets@gmail.com (M.V.Z.)

² Laboratory of Solid State Physics, The Institute of Nuclear Physics, Almaty 050032, Kazakhstan

³ Department of General Physics, Satbayev University, Almaty 050032, Kazakhstan

⁴ Department of Solid State Physics, Belarusian State University, 220050 Minsk, Belarus

* Correspondence: kayrat.kadyrzhanov@mail.ru; Tel./Fax: +77-024-4133-68

Abstract: This research investigated how changes in the composition of Nb–Ti–V–Zr-based alloys affect their resistance to radiation damage and the preservation of strength characteristics when exposed to the heavy ions Kr¹⁵⁺ and Xe²³⁺. These heavy ions simulate the impact of nuclear fuel fission fragments on the material. The primary objective of this study was to explore how variations in alloy components influence radiation resistance and the retention of alloy strength properties. Accumulation of radiation defects can potentially lead to embrittlement and a decrease in resistance to external factors during operation. An analysis of the X-ray diffraction data obtained from the initial alloy samples, in relation to the variations in the number of components, revealed that an increase in the number of components leads to the formation of a denser crystal structure. Additionally, this resulted in the emergence of a dislocation strengthening factor associated with changes in crystallite size. Concurrently, when assessing changes in the strength characteristics of the irradiated alloys, it was observed that the NbTiV and NbTiVZr alloys demonstrated the highest resistance to strength property degradation, specifically a 2.5- to 5-fold increase in resistance against a significant decrease in hardness. It was confirmed that the significant factor contributing towards the enhancement and preservation of the structural and strength properties is the dislocation strengthening mechanism. An increase in dislocation strengthening effectively enhances resistance against destructive embrittlement, particularly when exposed to high-dose irradiation.

Keywords: radiation-induced damage; disorder; softening; swelling; radiation resistance; strength; high-entropy alloys



Citation: Giniyatova, S.G.; Kadyrzhanov, K.K.; Shlimas, D.I.; Borgekov, D.B.; Uglov, V.V.; Kozlovskiy, A.L.; Zdorovets, M.V. Effects of Structural Radiation Disorder in the Near-Surface Layer of Alloys Based on NbTiVZr Compounds Depending on the Variation of Alloy Components. *Crystals* **2023**, *13*, 1543. <https://doi.org/10.3390/cryst13111543>

Academic Editor: Weichao Bao

Received: 28 September 2023

Revised: 21 October 2023

Accepted: 24 October 2023

Published: 27 October 2023



Copyright: © 2023 by the authors. Licensee MDPI, Basel, Switzerland. This article is an open access article distributed under the terms and conditions of the Creative Commons Attribution (CC BY) license (<https://creativecommons.org/licenses/by/4.0/>).

1. Introduction

Currently, one of the promising areas of research in the field of materials science focuses on the exploration of the potential for developing and assessing resistance to various external factors, including radiation damage and high-temperature corrosion, in multi-component alloys. This includes high-entropy alloys, which are primarily composed of refractory metals, like vanadium, titanium, niobium, zirconium, and others [1–5]. The selection of alloy components is typically guided by their physicochemical, thermophysical, and mechanical properties. The combination of these characteristics within the alloy's framework allows for the creation of materials with superior performance compared to pure metals, even refractory ones [6–8]. Furthermore, using a combination of elements, like Nb–Ti–V–Zr, allows for the fabrication of alloys with low density, typically less than 7 g/cm³, while still exhibiting exceptional resistance to a range of external factors, such as mechanical stresses, corrosion-induced deformations, radiation damage, and more [9,10].

It is noteworthy that in the process of selecting specific combinations of alloy constituents, a considerable amount of emphasis is placed on their individual characteristics and their capacity to form stable structural compounds when blended together. In recent years, there has been a growing focus on research endeavors dedicated to assessing the radiation resistance of these alloys and examining how variations in alloy components affect their ability to withstand and mitigate the effects of radiation-induced damage [11–13]. Consequently, several studies [13–16] have demonstrated that augmenting the number of alloy constituents results in an enhanced resistance of structural and strength properties against the accumulation of radiation-induced damage. Researchers have attributed this phenomenon to the presence of boundary effects, the strengthening effects of dislocations, and the intrinsic stability conferred by the alloy constituents themselves [17,18]. Additionally, a considerable level of attention has been dedicated to research endeavors focused on simulating radiation damage under conditions closely resembling real operational conditions. This approach aimed to establish criteria for the suitability of these alloys as structural materials based on the insights gleaned from such investigations [19,20].

The primary objective of this study was to scrutinize the mechanisms of structural radiation damage occurring in the near-surface layer of alloys composed of NbTiVZr compounds when subjected to irradiation with the heavy Kr¹⁵⁺ and Xe²³⁺ ions. Furthermore, another aim was to discern the connection between the number of alloy constituents and their resistance to radiation-induced damage, culminating in subsequent deterioration due to the accumulation of radiation effects. The selection of heavy ions, namely Kr¹⁵⁺ and Xe²³⁺, alongside irradiation fluences within the range from 10¹⁰ to 10¹⁵ ion/cm², serves to replicate the impacts akin to fission fragments originating from nuclear fuel within a reactor core. This endeavor, in turn, facilitates the assessment of the viability of employing these alloys as structural materials in nuclear reactors [21,22]. The radiation-induced corrosion processes occurring in the surface layer of alloys pose the most significant threat to their operational efficiency. The accumulation of radiation-induced damage within the near-surface layer has the potential to give rise to metastable regions characterized by elevated levels of deformation distortions and residual stresses. The presence of these regions has an adverse impact on the mechanical properties of the alloys [23,24]. Conversely, altering the alloy's composition by increasing the number of components may result in the creation of inter-boundary effects that hinder the growth of defective regions within the damaged layer. The appeal of multi-component alloys, including high-entropy alloys centered on refractory metals, consists of their substantial potential as substitutes for steels, which are traditionally employed as structural materials in high-temperature nuclear reactors.

2. Materials and Methods

2.1. Synthesis and Characterization of the Structural and Phase Compositions of the Studied Samples

Alloys based on NbTiVZr compounds were chosen as the subject of this investigation, with variations involving a gradual increase in the number of components within the compound (i.e., Nb, NbTi, NbTiV, and NbTiVZr). The selection of these alloy types for the study of resistance to radiation damage and the subsequent accumulation of structural radiation defects leading to disorder and destruction was based on the combined properties of these compounds. These alloys offer the advantage of achieving high strength and resistance to external stresses, along with the capability to effectively operate under conditions of elevated temperatures and background radiation (this refers to the study of gamma radiation in the form of fission fragments of nuclear fuel). The samples were fabricated by altering the proportions of chemically pure (99.9%) Nb, Ti, V, and Zr components through vacuum arc melting under pressure. To ensure a uniform element distribution within the alloy volume, the melting process was repeated a minimum of 5 times. Consequently, a range of alloys with varying component ratios, including equiatomic compositions and different densities, were produced.

Figure 1 presents the outcomes of the X-ray phase analysis conducted on the alloys, considering variations in the number of components. The diffraction patterns were acquired using Bragg–Brentano geometry within the angular range of $2\theta = 30\text{--}100^\circ$, with a 0.03° increment. These diagrams were generated using a D8 Advance ECO diffractometer (Bruker, Berlin, Germany). During the process of data recording, the sample holder rotated around its axis at a rate of 10 revolutions per second to mitigate the impact of sample orientation on the holder, which could lead to texturing effects. The phase composition analysis, along with the refinement of the crystal lattice parameters and volume, was executed using the DiffracEVA v.4.2 software code (Bruker, Berlin, Germany). The crystal lattice parameters and interplanar distances were refined through referencing card values from the PDF-2 (2016) database. The determination of crystallite sizes (L) and dislocation density ($\delta = 1/L^2$) involved estimating the FWHM value for all the observed diffraction maxima. Subsequently, the Scherrer method was applied, accounting for deformation factors that influenced FWHM broadening. The resulting parameter calculations are presented in Table 1.

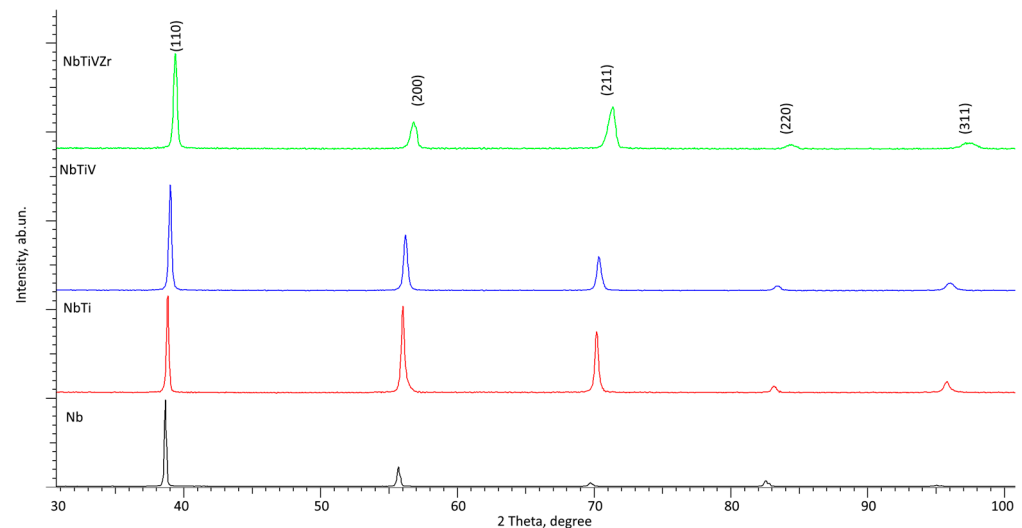


Figure 1. The results of X-ray diffraction of the studied alloy samples depending on the variation of components in the composition (Nb, NbTi, NbTiV, and NbTiVZr).

Table 1. Data on the crystal lattice parameters of alloys depending on component variations.

Parameter	Nb	NbTi	NbTiV	NbTiVZr
Lattice parameter, Å	3.2936 ± 0.0036	$a = 3.2789 \pm 0.0016$	$a = 3.2643 \pm 0.0017$	$a = 3.2322 \pm 0.0025$
Volume lattice, Å ³	35.73 ± 0.05	35.25 ± 0.04	34.76 ± 0.3	33.77 ± 0.5
Crystalline size (L), nm	52.4 ± 0.5	46.7 ± 0.3	40.8 ± 1.1	30.7 ± 0.9
Dislocation density ($\delta = 1/L^2$), cm ⁻²	0.36×10^9	0.46×10^9	0.61×10^9	1.06×10^9
Density, g/cm ³	8.634	6.629	6.039	6.955

Analysis of the X-ray phase data revealed that in the case of a single-component alloy primarily composed of niobium, the observed diffraction reflections, their angular position, and intensity corresponded to the Nb phase. This phase exhibited a body-centered crystal lattice, with an $Im\bar{3}m(229)$ spatial system and crystal lattice parameter $a = 3.2936 \pm 0.0036$ Å, which slightly deviates from the reference value of $a = 3.3033$ Å (PDF-00-034-0370). According to the data obtained, this alloy was characterized by the dominance of one textural direction (110), the intensity of the reflection of which was several times higher than the intensity of the other reflections. The addition of titanium to

the alloy, in order to obtain a two-component NbTi alloy with an equiatomic composition, also led to the formation of a body-centered NbTi phase (PDF-01-071-9955). However, the shifts in the diffraction maxima in comparison with a single-component Nb alloy characterized a decrease in the parameters of the crystal lattice (see the data in Table 1), as well as its compaction. This change can be explained by the difference in the ionic radii of the titanium and niobium ions. Moreover, in contrast to the one-component Nb alloy, which was characterized by one dominant textural direction, NbTi was characterized by an almost equally probable distribution of grain orientation along three texture directions, namely (110), (200), and (211).

The introduction of vanadium into the alloy resulted in a noticeable shift in the diffraction reflections towards higher angles, indicating a compression of interplanar distances and a reduction in the crystal lattice parameters. Furthermore, in the two- and three-component alloys, alongside the shift in the diffraction reflections, there was also an observable broadening of the diffraction lines. This broadening is indicative of reduced crystallite sizes, leading to a growth in dislocation density and the proliferation of grain boundaries.

Regarding the four-component NbTiVZr alloy, the X-ray diffraction patterns exhibited a significant shift in the position of the reflections compared to the maxima for the Nb alloy. Furthermore, there was a minor reduction in the crystal lattice parameters, amounting to less than a 2% decrease when compared to the parameter for the Nb alloy. Notably, unlike the two- and three-component alloys, the NbTiVZr alloy displayed two distinct textural directions, namely (110) and (211). Additionally, there was a substantial broadening of the FWHM value, which is indicative of a reduction in the crystallite sizes by over 40% when compared to the sizes observed in the Nb alloy. A comparable pattern, linked to a denser crystal lattice in the NbTiVZr alloy when contrasted with the two- and three-component alloys, was documented in a previous study [25]. In that study, the authors associated this phenomenon with the strengthening effects observed in alloys as the number of components increased.

Furthermore, all the alloys that were obtained, irrespective of the number of components they contained, exhibited a body-centered crystal structure of the $Im\bar{3}m(229)$ space group. It is worth mentioning that altering the number of alloy components results in a reduction in its density. In the case of NbTiVZr, this led to the creation of a high-entropy alloy based on refractory compounds, with a low density of approximately 6.5 g/cm³.

The analysis of alterations in the crystallite sizes and dislocation density revealed the occurrence of a phenomenon known as dislocation strengthening. When transitioning from a single-component Nb alloy to a two-component NbTi alloy, this strengthening effect amounted to over 27%. In the case of the three-component alloy, it exceeded 60%, and for the high-entropy NbTiVZr alloy, dislocation strengthening was more than 2.5 times greater than that observed in the single-component Nb alloy. The formation of such structures enhances resistance to cracking and hardening, resulting in increased hardness and crack resistance.

2.2. Irradiation of Alloys with Heavy Ions to Simulate Radiation Exposure Comparable to That of Fission Fragments of Nuclear Fuel

To accomplish this objective, experimental procedures involved irradiating the chosen research specimens with the Kr¹⁵⁺ and Xe²³⁺ heavy ions at fluences ranging from 10¹⁰ to 10¹⁵ ion/cm² and energies spanning from 150 to 230 MeV. The samples were irradiated in the DC-60 heavy ion accelerator (Institute of Nuclear Physics of the Ministry of Energy of the Republic of Kazakhstan, Astana, Kazakhstan). Heavy ion irradiation was performed under the following parameters. For the Kr¹⁵⁺ ions, the training energy was chosen to be 150 MeV; for the Xe²³⁺ ions, the irradiation energy was chosen to be 230 MeV.

The choice of the type of heavy ions, specifically Kr¹⁵⁺ and Xe²³⁺, was based on their capacity to simulate the mechanisms of radiation-induced damage similar to fission fragments, comparable to reactor tests, which made it possible to evaluate the possibilities

of using the selected alloy compositions as reactor materials. It is worthy to note that the use of these types of ions makes it possible to simulate radiation damage and the kinetics of their accumulation in the near-surface layer of alloys, about 10–15 μm thick, which is most susceptible to external influences both in the case of reactor tests and mechanical influences. In order to estimate the magnitude of energy losses, as well as the maximum travel depth of the ions in the alloys, calculations were carried out using the SRIM Pro 2013 program code. Regarding the assessment of ionization losses, with respect to variations in the alloy components, the values of dE/dx_{electron} were set in the range from 15 to 18 keV/nm for Kr^{15+} ion irradiation and from 20 to 25 keV/nm for Xe^{23+} ion irradiation. Additionally, the values of dE/dx_{nuclear} were approximately from 0.3 to 0.6 keV/nm for the Kr^{15+} ions and from 0.5 to 0.7 keV/nm for the Xe^{23+} ions. In this context, the maximum ion penetration depth into the material was estimated to be in the range from 11 to 12 μm when irradiated with the Kr^{15+} ions and from 15 to 16 μm for the Xe^{23+} ions.

2.3. Methodology for Measuring the Strength Characteristics and Resistance to High-Temperature Degradation

The assessment of the strength properties of alloys concerning the variation in the number of components and the alterations induced via heavy ion irradiation was conducted using the hardness determination method through indentation. A Vickers diamond pyramid was used as the indenter, and measurements were executed via a LECO LM700 microhardness tester (LECO, Tokyo, Japan). The choice of measurement parameters, including a load of 100 N on the indenter, was experimentally determined to account for the impact of structural modifications within the damaged layer, which had an approximate thickness of 10–15 microns. The assessment of resistance to the degradation in the strength characteristics was carried out via comparative analysis of alterations in hardness values before and after a series of measurements for the initial and irradiated samples. The hardness of the samples was measured using the indentation method, and the measurements were carried out in the form of serial tests over the entire area of the sample in order to determine the uniformity and isotropy of the observed changes associated with softening.

Experiments to evaluate thermal stability and resistance to high-temperature degradation were conducted on a set of samples in their original (unirradiated) condition, as well as after irradiation with the Kr^{15+} and Xe^{23+} ions at a fluence of 10^{15} ions/cm². Test conditions were selected to simulate oxidation processes under a high-temperature air atmosphere. The temperature range spanned from 700 to 1000 °C, with increments of 100 °C. The samples were subjected to heating in a muffle furnace within an air atmosphere, with a heating rate of 50 °C/min. They were held at this temperature for 500 h to initiate the high-temperature degradation process, after which the samples were cooled, and their strength characteristics were measured using the indentation method.

3. Results and Discussion

3.1. Comparative Analysis of Changes in the Structural Disorder of a Damaged Alloy Layer upon Irradiation with Heavy Ions

The assessment of structural disorder, which was influenced by the type of external factors (such as varying the type of irradiation ions and fluence), involved calculating the extent of deformation-induced distortion in the crystal lattice volumes of the samples under irradiation compared to their initial values before irradiation. Additionally, the concentration of defective regions within the damaged layer was calculated. These calculation results are presented in Figures 2 and 3. The swelling value was ascertained by evaluating the alterations in the crystal lattice volume before and after irradiation, and this evaluation depended on the irradiation fluence. The deformation factor was determined by examining the changes in the crystal lattice parameters before and after irradiation. When calculating the swelling values and the concentration of defective inclusions in the specimens, their penetration depths were considered by measuring their X-ray diffraction patterns followed by their subsequent analyses.

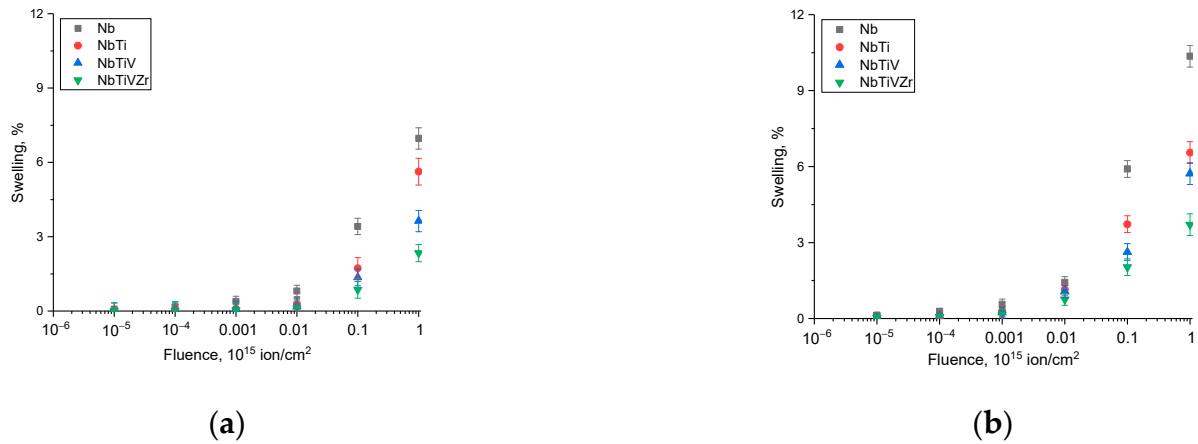


Figure 2. The results of deformation distortions of the crystal lattice volume (ΔV) depending on the type of ions and irradiation fluence: (a) when irradiated with Kr¹⁵⁺ ions, and (b) when irradiated with Xe²³⁺ ions.

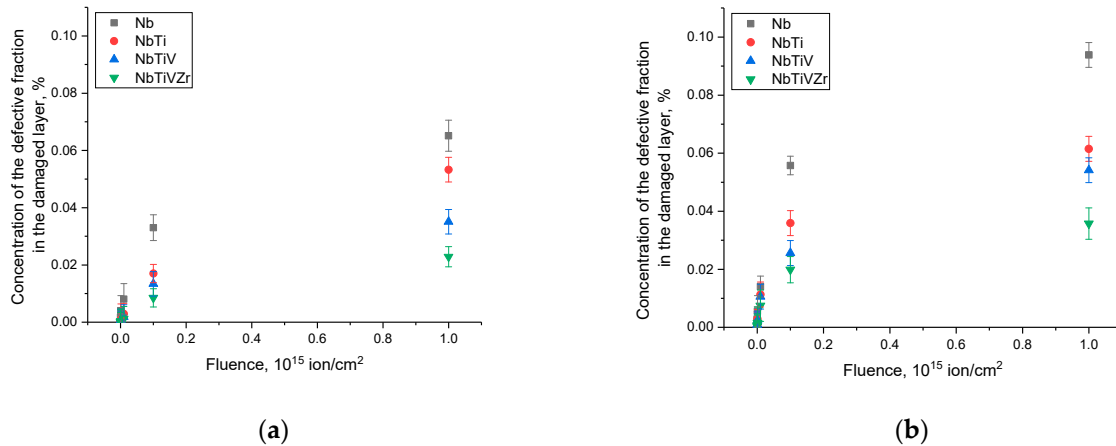


Figure 3. The assessment results of the defective fraction concentration in the damaged alloy layer volume under varying irradiation conditions: (a) when irradiated with Kr¹⁵⁺ ions, and (b) when irradiated with Xe²³⁺ ions.

The overall pattern of alterations in the structural parameters, particularly the expansion of the crystal lattice, suggests the emergence of isotropic tensile strain distortions within the structure. These distortions cause an increase in the crystal structure's parameters and volume. The isotropic nature of these distortions arises from the body-centered crystal lattice type, wherein any deformation distortion is equally likely to result in a lattice volume change. Additionally, it is important to highlight that the nature of these structural modifications, such as the expansion of the crystal lattice, exhibits a non-linear relationship with the irradiation fluence. The most significant alterations were only observed within the fluence range from 10^{14} to 10^{15} ion/cm². This pattern of changes in the deformation distortion of the crystal structure can be elucidated by considering the cumulative effect linked to the growing irradiation fluence. Consequently, this results in an increased level of structural damage caused by the interaction between the incident ions and the alloys' crystal structure. In this case, when exposed to low irradiation fluences (10^{10} – 10^{12} ion/cm²), the formation of structurally deformed regions within the alloys, along the path of the ions, exhibited localized characteristics, with dimensions on the order of 5–10 nm in diameter. This localized nature of deformation arose due to the random and chaotic nature of the irradiation process, leading to a relatively low likelihood of two ions simultaneously hitting the same point. Additionally, the isolated structurally deformed regions within the damaged layer were primarily attributed to ionization processes involving the redistribution of electron density

and the creation of vacancy or point defects, most of which have the potential to undergo annihilation following irradiation. Consequently, within the structure of the damaged layer at these specific irradiation fluences, minor structural alterations were detected, signifying an increase in the crystal lattice volume. Moreover, the concentration of defective inclusions remained below 0.01%. The impact of ionization losses stemming from the incident ions and the related processes they trigger on the extent of radiation-induced damage was not only evident at high fluences but also at lower ones (10^{10} – 10^{12} ion/cm²). This phenomenon became particularly apparent in a comparative analysis of structural changes when irradiated with the Kr¹⁵⁺ and Xe²³⁺ ions. Under low irradiation fluences (10^{10} – 10^{12} ion/cm²), a noticeable rise in the concentration of the defective fraction was apparent when irradiated with Xe²³⁺ ions, especially in the case of single-component alloys, which, when subjected to an overall analysis of observed alterations, displayed the least resistance to external influences. As irradiation fluence grew beyond 10^{12} – 10^{13} ion/cm², there was a significant spike in the concentration of the defective fraction within the damaged layer. Concurrently, there was an elevation in deformation within the volume of the crystal lattice, signifying an accelerated destructive alteration in the crystal structure of the damaged layer. These alterations can be elucidated by considering the accumulation of structural distortions and the amalgamation of previously isolated structurally deformed regions into larger clusters or complex defects due to heightened density (research has shown that at fluences exceeding 10^{12} ion/cm², there is an overlapping effect). Additionally, more conspicuous structural modifications in the samples when exposed to the heavy Xe²³⁺ ions at the same fluences indicated disparities in the values of the structural distortions. These distortions formed along the path of ion movement within the material during their interaction with incoming ions and manifested as increased dimensions compared to analogous changes induced via irradiation with Kr¹⁵⁺ ions. Simultaneously, these discrepancies were predominantly attributed to the ionization losses incurred by incident ions during their interactions with the electron shells. This interaction engenders heterogeneities in the distribution of electron density, and as a result, ionization processes give rise to the creation of residual mechanical stresses. These residual mechanical stresses manifested as deformation distortions within the crystal structure, which are linked to ionization processes [26–29]. An elevation in the concentration of residual mechanical stresses within the structure of the damaged layer precipitated hastened degradation, manifesting as volumetric swelling of the crystal lattice. This swelling was associated with deformation distortions at interplanar distances and the formation of vacancy defects.

Figure 4a presents a comparative assessment of alterations in the expansion of the crystal lattice in the examined alloys when subjected to the highest irradiation fluence, which signifies the deformation distortions and radiation-induced disordering within the damaged layer. Examination of the collected data revealed a more pronounced structural distortion and an accumulation of deformation-related structural distortions in the alloy specimens exposed to the heavy Xe²³⁺ ions. For instance, in the case of the Nb alloys, the extent of structural distortion, represented via lattice expansion, when subjected to the heavy Kr¹⁵⁺ and Xe²³⁺ ions, with a fluence of 10^{15} ion/cm², was 7.0% and 10.3%, respectively. In the case of the NbTi alloys, these figures were approximately 5.6% and 6.7% when exposed to the heavy Kr¹⁵⁺ and Xe²³⁺ ions, respectively. As for the NbTiV alloys, these metrics stood at 3.6% and 5.7% for the heavy Kr¹⁵⁺ and Xe²³⁺ ions, respectively. Notably, the NbTiVZr alloy samples exhibited the highest resistance to swelling, with swelling values of 2.3% and 3.7% at an irradiation fluence of 10^{15} ions/cm² when exposed to the heavy Kr¹⁵⁺ and Xe²³⁺ ions, respectively. When comparing the swelling levels across different alloys, it was evident that, in comparison to the Nb alloy, the resistance to deformation distortions resulting from irradiation was approximately 20%, 50%, and 70% higher for the NbTi, NbTiV, and NbTiVZr alloys, respectively.

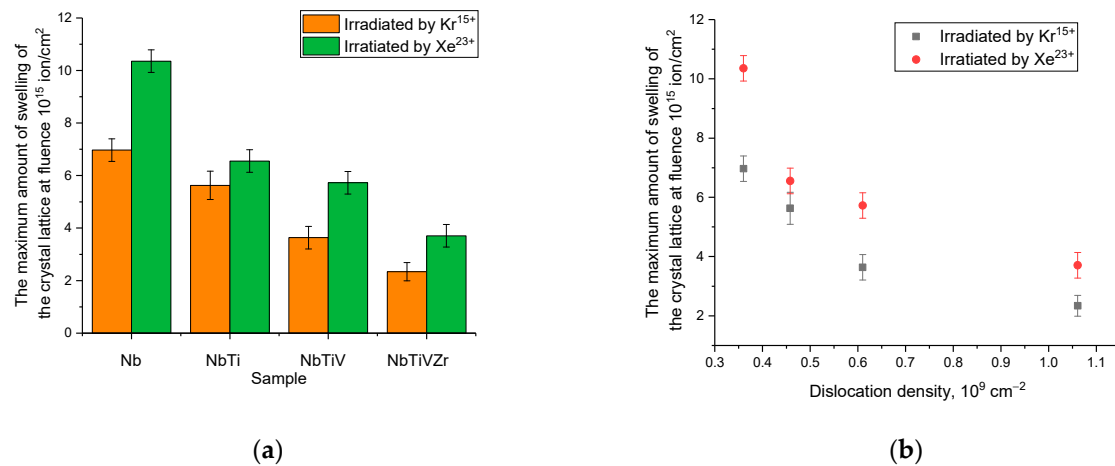


Figure 4. (a) The results of a comparative analysis of changes in the swelling values of the crystal lattices of the alloys under study at a maximum irradiation fluence of 10^{15} ion/cm²; (b) effect of dislocation density on resistance to degradation swelling under irradiation, with a maximum irradiation fluence of 10^{15} ion/cm².

One of the key factors contributing to the enhanced resistance against detrimental lattice swelling caused via the accumulation of radiation-induced damage and tensile strain distortions can be attributed to alterations in the dislocation density within the alloys, particularly with an increase in the number of components in their composition. This leads to the establishment of additional boundary effects that act as safeguards against severe distortion during high-dose irradiation. Figure 4b illustrates the outcomes of a comparative analysis of dislocation density changes in alloys as a function of the number of components in their composition, focusing on their resistance to swelling at the maximum irradiation fluence of 10^{15} ion/cm². These data presented clearly demonstrate a direct relationship between resistance to swelling and variations in the dislocation density. In other words, when the samples exhibit higher dislocation densities (which occur due to changes in the number of alloy components), the surface layer's structure exposed to irradiation experiences fewer structural distortions and tensile deformations. The accumulation of these distortions is what ultimately leads to swelling and material degradation.

When considering the application of these alloys as structural materials subjected to ionizing radiation, especially irradiation with heavy ions similar in energy to nuclear fuel fission fragments, understanding the kinetics of radiation damage accumulation and crystal structure deformation is a crucial factor in assessing their potential and possible uses. The acquired data revealed that altering the alloy's composition results in an improved resistance to consequences like deformation swelling, which arises from the accumulation of radiation-induced damage in the surface layer. This rise in stability and resistance to radiation swelling was due to the following factors. Firstly, a change in the amount of components in the alloys leads to the emergence of additional inter-boundary effects associated with the formation of smaller grains, which, in turn, leads to an increase in the dislocation density, a change which leads to strengthening and increased resistance to swelling. Also, the presence of inter-boundary effects associated with grain sizes led to the appearance of additional defect sinks, which leads to an increase in the number of annihilated point defects and vacancies at the sink boundary. The review published by Zhang, Z., et al. [30] provides a thorough description of the effect of grain boundaries and dislocation strengthening in high-entropy alloys. The findings and explanations within this review are consistent and elucidate the structural modifications observed in this study. These changes were linked to an enhanced resistance to radiation swelling, which correlated with a rise in the number of components in the alloy. Furthermore, as indicated by Xia S. Q. et al. [31], altering the type of high-entropy alloy results in an improved resistance to radiation embrittlement due to the specific crystal's structure and

its remarkable stability against external influences. The established relationships between changes in the dislocation density and the extent of structural disorder (swelling) reveal the beneficial impact of dislocation strengthening. This effect was linked to the reduction in grain size and, consequently, the emergence of numerous inter-boundary influences that impede the migration of vacancy and point defects. These inter-boundary effects also create additional hindrances to the deformation distortion of the crystal's structure.

3.2. Effect of Irradiation with Heavy Ions on Changes in the Strength Properties of the Alloys

Figure 5 presents the findings related to variations in the hardness of alloy samples under different external influences. These observed trends depict the decline in hardness values as radiation damage accumulated and structural disorder occurred, with increasing irradiation fluence.

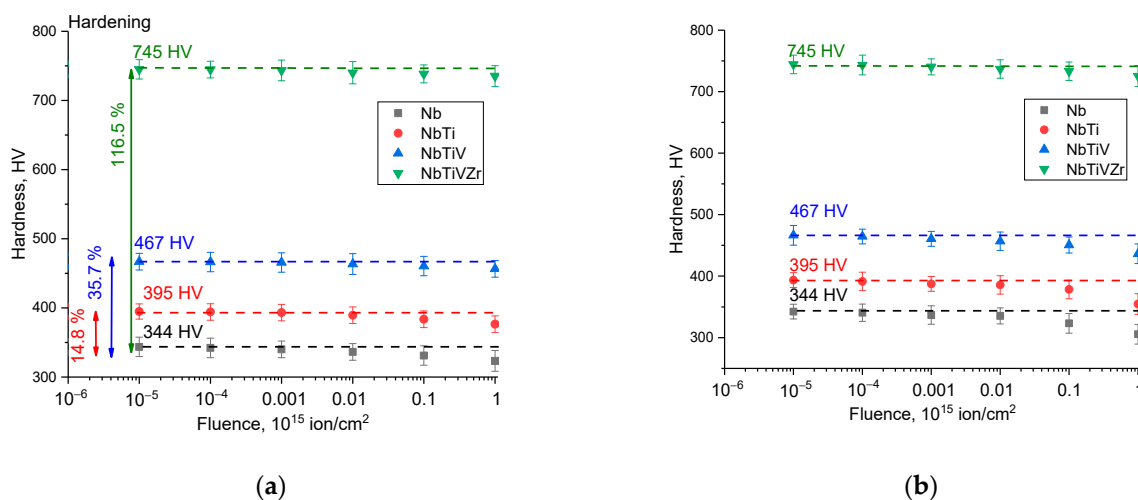


Figure 5. The results of alterations in the hardness of alloys depending on the irradiation fluence and the type of incident ions: (a) when irradiated with Kr^{15+} ions; (b) when irradiated with Xe^{23+} ions (the dotted lines in these figures indicate the hardness values for the original samples that were not subjected to irradiation; figure (a) illustrates the results of hardening the alloys with varying components. These lines were added to clearly demonstrate changes in the hardness values in comparison with their initial values, indicating a softening of the alloys).

The overall trends in the alterations of hardness in the studied alloys exhibited clear dependencies on both the type of ion exposure (i.e., the type of ions) and the irradiation fluence. Furthermore, it is crucial to consider the alloy's composition when analyzing the changes in hardness. Evaluations of hardness modifications associated with varying components revealed the following: the addition of titanium to an alloy resulted in a 14.8% increase in hardness, introducing vanadium to a two-component alloy led to a 35.7% hardness increase, and in the case of the NbTiVZr alloy, there was a remarkable hardness increase of over 116% when compared to the Nb alloy. Moreover, these changes in hardness for the initial samples have a good correlation with the data on changes in the dislocation density, which indicates the formation of the so-called effect of dislocation hardening of alloys, with variations in the number of components in them.

Examining alterations in the hardness values of alloys with increasing irradiation fluence revealed that the most substantial changes occur when the irradiation fluence surpasses 10^{13} ion/cm² when exposed to the Kr^{15+} ions and exceeds 10^{12} ion/cm² when exposed to the Xe^{23+} ions. In this scenario, the observed trend of changes, specifically the decline in hardness values at equivalent irradiation fluences for various ions, signifies a more pronounced softening of the alloys during irradiation with Xe^{23+} ions. In this context, altering the type of ions from Kr^{15+} to Xe^{23+} during irradiation resulted in a more significant 1.5- to 2.0-fold reduction in resistance to softening under the same irradiation fluences. This phenomenon may stem from substantial structural modifications induced

via Xe^{23+} irradiation during the interaction between the incident ions and the alloy's crystal lattice, coupled with substantial ionization losses that can trigger changes across a larger volume compared to Kr^{15+} ion irradiation (referring here to differences in the diameters of structurally deformed regions formed along the trajectory of ion movement within the damaged layer). It is worth highlighting that as the number of components in the alloys increases, it not only results in a higher initial hardness but also a greater resistance to softening under high-dose irradiation. In the instance of the NbTiV and NbTiVZr alloys, the resistance to softening at the maximum irradiation fluence exceeded the value for the Nb alloy by more than 3–5 times, demonstrating the beneficial impact of the dislocation strengthening factor on enhancing stability against softening.

Figure 6 presents comparative data on the dependence of the changes in softening (decrease in hardness) on the degree of structural disorder, with changes in the irradiation fluence and the type of incident ions. The softening degree was assessed by comparing the obtained data on the hardness of the samples in the initial state with the irradiated data, followed by conversion into a percentage.

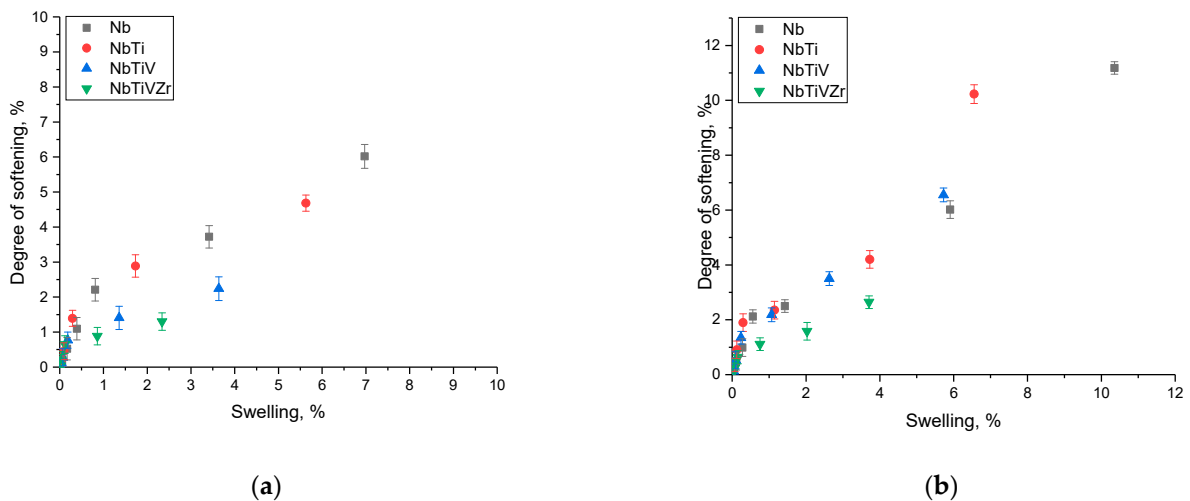


Figure 6. Dependence of changes in the softening degree (decrease in hardness) on the value of structural disorder: (a) when irradiated with Kr^{15+} ions, and (b) when irradiated with Xe^{23+} ions.

The overall pattern of the depicted relationships between the extent of softening (hardness decrease) and the level of structural changes resulting from deformation-induced distortions of the crystal structure (i.e., its swelling due to deformation) demonstrates a close alignment of the data. When the swelling of the crystal lattice was minimal, signifying isolated structurally deformed regions (at low fluences of 10^{10} – 10^{12} ion/cm²), the decline in the strength properties was also minimal, typically less than 0.5–1%. Simultaneously, the occurrence of what is referred to as dislocation strengthening within the alloy compositions, as the number of components increases, resulted in a heightened resistance to a significant reduction in hardness and softening of the alloys. For the four-component alloys, this translated into a reduction of over five times in the degree of disorder compared to similar alterations observed in a Nb alloy at the maximum irradiation fluences of the Kr^{15+} and Xe^{23+} heavy ions. The critical thresholds for structural characteristic alterations, beyond which a noticeable decline in strength properties becomes evident, were associated with a 4–5% enlargement in the crystal lattice volume. Upon surpassing these thresholds, a marked deterioration in strength properties and a reduction in crack resistance became apparent. Additionally, the ionization losses incurred during the interaction between the incident ions and the crystal structure play a significant role in this context. Under irradiation with Xe^{23+} ions, the degradation in strength characteristics occurred at a considerably accelerated rate compared to irradiation with Kr^{15+} ions. This was evident in the fluctuating dynamics of strength characteristics and their fluctuations relative to the

degree of structural disorder. Notably, this effect was most pronounced in the one- and two-component alloys. Conversely, in the case of the NbTiV and NbTiVZr alloys, this effect was less conspicuous. This discrepancy can be attributed to the dislocation strengthening factor, which impedes microcrack propagation within the structure, erecting barriers in the form of boundary effects and dislocation loops.

The hardening effects observed for the NbTiV and NbTiVZr alloys were due to their increased resistance to radiation-induced swelling associated with the accumulation of radiation damage (including point defects, vacancies, and primary knocked-out atoms). In this case, the hardening effects observed for these alloys, with increasing irradiation fluence (as well as with changing the type of ions during irradiation), are in good agreement with several experimental works [32,33], in which this hardening was explained by dislocation strengthening. In the case of a high dislocation density, as well as the presence of inter-boundary effects (associated with small grain sizes), the propagation of microcracks in the structure under external loads is difficult, which leads to an increase in resistance to embrittlement and destruction of strength properties. Notably, as illustrated in Figure 6, the most pronounced hardening effect was observed in the NbTiVZr alloys. These alloys possess an equiatomic distribution of elements in their structure, which contributes to an elevated resistance to embrittlement and destruction, as elaborated in the studies published by the authors of [30–32].

3.3. Evaluation Results of the Studied Alloy Samples for Thermal Heating Resistance

An essential criterion for assessing the durability of alloys under operational conditions is the retention of their strength properties when subjected to elevated temperatures, typically in the range from 700 to 1000 °C. Elevated temperatures can potentially result in a detrimental alteration of the alloys' strength characteristics due to specific processes, such as oxidation or volumetric thermal expansion. Such a decline in hardness can exert adverse consequences for the subsequent performance of the alloys and the products derived from them. In the case of using these alloys as structural materials for high-temperature nuclear reactors, which have the greatest prospects for the development of the nuclear industry in the coming decades, the stability of the alloys and the preservation of the stability of structural and strength properties under high-temperature operating conditions is one of the key factors. Under high-temperature operating conditions (700–1000 °C), the crystal lattice of the alloy undergoes additional changes associated with an increase in the intensity and amplitude of thermal vibrations of atoms, which, together with the accumulation of radiation damage, can lead to accelerated degradation and embrittlement of the damaged layer. In this case, accelerated degradation can result in a decline in the strength characteristics, which will adversely affect the resistance to external mechanical influences.

It is noteworthy that, despite niobium's considerable promise in materials science, niobium-based alloys are particularly susceptible to high-temperature degradation, primarily due to niobium's pronounced oxidizing tendencies when exposed to elevated temperatures. Figure 7 displays the outcomes regarding variations in the hardness values observed in the studied alloy samples before and after undergoing tests for thermal stability, while being subjected to thermal heating within the temperature range from 700 to 1000 °C. The overall trend evident from these relationships underscores the adverse impact of thermal heating, resulting in a reduction in the strength characteristics, as reflected by a decline in the hardness values in the examined samples as the heating temperature rose. Notably, the alloys based on niobium (Nb) exhibited the least resistance to these influences, and both the original (non-irradiated) samples and the irradiated ones exhibited a rather steep reduction in their hardness values with growing test temperature. Concerning the initial samples of the NbTi, NbTiV, and NbTiVZr alloys, the most notable decline in hardness was only noticeable at temperatures surpassing 800 °C. This observation underscores the beneficial impact of incorporating additional components in enhancing resistance to high-temperature degradation. In the case of the irradiated samples, this decline was more pronounced, signifying the influence of accumulated structural distortions in the damaged

layer on the decreased resistance to high-temperature degradation. The analysis of the acquired data revealed a direct correlation between the initial structural distortions in the irradiated samples (with variations in ion types) and the extent of hardness reduction during high-temperature stability assessments. In instances where structural distortions were minimal, as seen in the NbTiV and NbTiVZr alloys exposed to Kr^{15+} ion irradiation, the decline in hardness was less significant compared to the samples that were subjected to Xe^{23+} ion irradiation, where the value of structural distortions (i.e., the degree of lattice swelling) was 1.5 to 2 times higher.

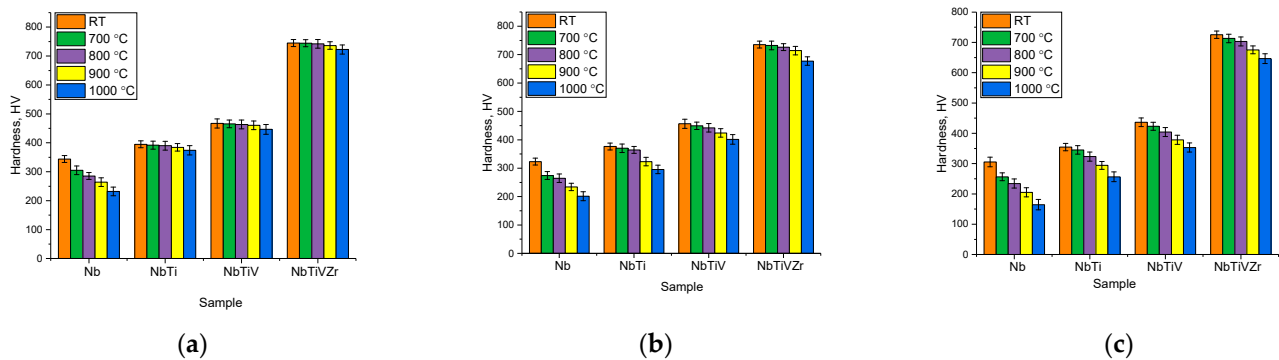


Figure 7. The assessment results of the hardness values of the alloys under study during high-temperature tests: (a) in the case of the initial samples, (b) when irradiated with Kr^{15+} ions, and (c) when irradiated with Xe^{23+} ions.

Using the data acquired from the alterations in hardness values during thermal resistance tests of the initial alloy specimens and those exposed to the heavy ions Kr^{15+} and Xe^{23+} , relationships illustrating the variations in the extent of hardness reduction for all samples under different thermal resistance conditions were formulated. The results of this comparative analysis can be seen in Figure 8. These data were obtained by comparing the hardness values measured before and after the high-temperature tests. This not only allowed for an assessment of the alloys' resistance to radiation damage but also for determination of the impact of accumulated radiation damage (deformation distortions in the crystal structure) on the maintenance of the strength properties during thermal heating. These findings were presented as graphs, showing the changes in the hardness reduction metrics for each type of sample studied, contrasting between the initial and irradiated samples.

As shown in the presented data, the Nb alloys, both in the original and irradiated states, proved to be the least resistant to high-temperature degradation. At the same time, the destructive changes in hardness for these alloys was primarily due to the low thermal stability of niobium, which can lead to its oxidation through the formation of an oxide layer on the surface, the thickness of which directly depends on the time and temperature of thermal exposure [34–36]. Moreover, in the case of the irradiated samples, the decrease in their hardness was about 30–50% at temperatures of 900–1000 °C, which indicates the low stability of the irradiated samples to high-temperature degradation, as well as its acceleration due to accumulated structural distortions in the damaged layer. In this case, as shown in the study published by the authors of [37], accelerated degradation can be caused via the formation of oxide layers on the surface, which, in the case of a near-surface layer damaged by irradiation, can contribute to its accelerated degradation and peeling, which leads towards a sharp deterioration in hardness.

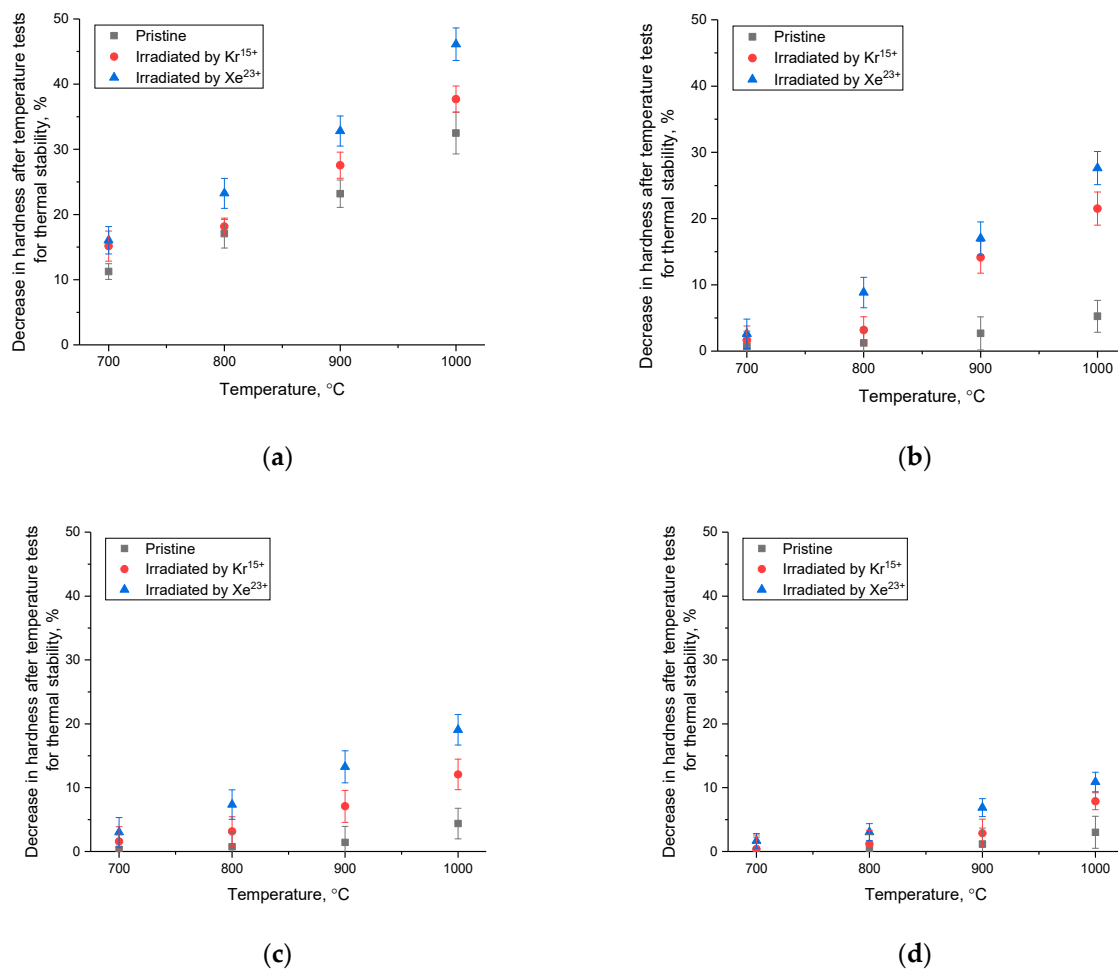


Figure 8. The assessment results of the decrease in hardness with varying temperatures of heat resistance tests in the case of the initial and irradiated samples: (a) the Nb alloy; (b) the NbTi alloy; (c) the NbTiV alloy; (d) the NbTiVZr alloy.

When considering the original samples, it became evident that the NbTiV and NbTiVZr alloys exhibited the highest resistance to thermal impacts. For these alloys, the rise in temperature from 700 to 900 °C did not result in substantial changes in their hardness values following the heat resistance tests. Even when subjected to thermal heating at 1000 °C, the reduction in hardness remained within the range of 3–4% compared to the initial values. However, in the case of the irradiated samples of the NbTiV and NbTiVZr alloys, a more pronounced decrease in hardness was observed at temperatures ranging from 800 to 1000 °C. This was attributed to the influences of accumulated structural distortions and residual mechanical stresses within the damaged layer, which, when subjected to external temperature influences, expedited the process of strength degradation. The heightened resistance to thermal degradation over prolonged periods exhibited by the NbTiV and NbTiVZr alloys can be attributed to their structural characteristics, which stem from the equiatomic distribution of elements within their structures. This distribution reduces the thermal oscillations of atoms within the crystal lattice, consequently resulting in an enhancement of the softening resistance.

Therefore, upon analyzing these dependencies, we can infer that when subjected to heavy ion irradiation with Kr¹⁵⁺ and Xe²³⁺, the NbTiV and NbTiVZr alloys experience a less pronounced acceleration of these processes, causing detrimental alterations in their strength properties. In contrast, the Nb and NbTi alloys exhibited accelerated surface degradation and a significant deterioration in the stability of their strength characteristics upon irradiation.

4. Conclusions

This study presented findings on the impact of altering the components of an Nb–Ti–V–Zr alloy on the resistance of structural parameters when exposed to the heavy Kr¹⁵⁺ and Xe²³⁺ ions, with energies of 150 and 230 MeV, respectively. The choice of irradiation conditions and ion types aimed to simulate radiation damage akin to the effects caused by fission fragments of nuclear fuel. Throughout this investigation, while analyzing the influence of varying alloy components compared to the initial Nb alloy, patterns of strengthening and structural ordering were identified, with an escalation in the number of components. Furthermore, in the case of the NbTiV and NbTiVZr alloys, strengthening was linked to alterations in the dislocation density. An increase in the dislocation density contributed to enhanced resistance against external factors, encompassing mechanical forces and the accumulation of radiation-induced damage. Simultaneously, during the examination of alterations in the alloys' strength characteristics when exposed to the heavy Kr¹⁵⁺ and Xe²³⁺ ions, it was observed that structural distortions resulting from the interaction between the heavy ions with the alloys' crystal structure manifested as tensile-type deformation residual stresses, which were most pronounced at higher irradiation fluences (above 10¹²–10¹³ ion/cm²). Throughout these investigations, it was determined that the observed enhancement in the resistance of the irradiated NbTiV and NbTiVZr alloys to the degradation in their strength characteristics was attributed to an increase in the resistance of the crystal structure against swelling, along with the effects of dislocation strengthening. In assessments of high-temperature degradation (through extended thermal exposure), it was revealed that the NbTiV and NbTiVZr alloys exhibited the greatest stability to thermal influences within the temperature range of 700–800 °C. This applied to both the initial and irradiated samples, not only underscoring their resistance to radiation-induced damage but also their potential for application in environments characterized by extremely high temperatures during operation.

In the future, based on the results obtained and a comparative analysis of the resistance of various types of alloys to radiation damage and their evolution under conditions of changing irradiation fluences, studies will be carried out aimed at determining the stability of alloy samples to radiation damage under irradiation conditions as close as possible to real operating conditions (irradiation at high temperatures, as well as irradiation with neutrons). The data obtained during these new experiments, as well as their comparison with the work already carried out, will make it possible to predict the potential for the use of these alloys as structural materials in nuclear energy.

Author Contributions: Conceptualization, S.G.G., V.V.U., D.I.S., D.B.B., K.K.K. and A.L.K.; methodology, V.V.U., S.G.G., M.V.Z. and A.L.K.; formal analysis, M.V.Z., D.I.S. and A.L.K.; investigation, S.G.G., V.V.U., M.V.Z., K.K.K., D.I.S. and A.L.K.; resources, A.L.K.; writing—original draft preparation, review, and editing, S.G.G., D.I.S. and A.L.K.; visualization, S.G.G. and A.L.K.; supervision, A.L.K. All authors have read and agreed to the published version of the manuscript.

Funding: This research was funded by the Science Committee of the Ministry of Education and Science of the Republic of Kazakhstan (No. BR18574135).

Data Availability Statement: Not applicable.

Conflicts of Interest: The authors declare no conflict of interest.

References

1. Senkov, O.N.; Senkova, S.V.; Miracle, D.B.; Woodward, C. Mechanical properties of low-density, refractory multi-principal element alloys of the Cr–Nb–Ti–V–Zr system. *Mater. Sci. Eng. A* **2013**, *565*, 51–62. [[CrossRef](#)]
2. Zhang, J.; Sun, F.; Hao, Y.; Gozdecki, N.; Lebrun, E.; Vermaut, P.; Prima, F. Influence of equiatomic Zr/Nb substitution on superelastic behavior of Ti–Nb–Zr alloy. *Mater. Sci. Eng. A* **2013**, *563*, 78–85. [[CrossRef](#)]
3. Karre, R.; Niranjana, M.K.; Dey, S.R. First principles theoretical investigations of low Young's modulus beta Ti–Nb and Ti–Nb–Zr alloys compositions for biomedical applications. *Mater. Sci. Eng. C* **2015**, *50*, 52–58. [[CrossRef](#)]

4. Ananchenko, D.V.; Nikiforov, S.V.; Kuzovkov, V.N.; Popov, A.I.; Ramazanov, G.R.; Batalov, R.I.; Novikov, H.A. Radiation-induced defects in sapphire single crystals irradiated by a pulsed ion beam. *Nucl. Instrum. Methods Phys. Res. Sect. B Beam Interact. Mater. At.* **2020**, *466*, 1–7. [[CrossRef](#)]
5. Kim, K.M.; Kim, H.Y.; Miyazaki, S. Effect of Zr content on phase stability, deformation behavior, and Young's modulus in Ti–Nb–Zr alloys. *Materials* **2020**, *13*, 476. [[CrossRef](#)] [[PubMed](#)]
6. Tseng, K.K.; Juan, C.C.; Tso, S.; Chen, H.C.; Tsai, C.W.; Yeh, J.W. Effects of Mo, Nb, Ta, Ti, and Zr on mechanical properties of equiatomic Hf–Mo–Nb–Ta–Ti–Zr alloys. *Entropy* **2018**, *21*, 15. [[CrossRef](#)]
7. Schneider, S.; Schneider, S.G.; Silva, H.M.D.; Moura Neto, C.D. Study of the non-linear stress-strain behavior in Ti–Nb–Zr alloys. *Mater. Res.* **2005**, *8*, 435–438. [[CrossRef](#)]
8. Liao, M.; Liu, Y.; Min, L.; Lai, Z.; Han, T.; Yang, D.; Zhu, J. Alloying effect on phase stability, elastic and thermodynamic properties of Nb–Ti–V–Zr high entropy alloy. *Intermetallics* **2018**, *101*, 152–164. [[CrossRef](#)]
9. Zheng, J.; Hou, X.; Wang, X.; Meng, Y.; Zheng, X.; Zheng, L. Isothermal oxidation mechanism of Nb–Ti–V–Al–Zr alloy at 700–1200 °C: Diffusion and interface reaction. *Corros. Sci.* **2015**, *96*, 186–195. [[CrossRef](#)]
10. Zhang, Y.; Silva, C.; Lach, T.G.; Tunes, M.A.; Zhou, Y.; Nuckols, L.; Weber, W.J. Role of electronic energy loss on defect production and interface stability: Comparison between ceramic materials and high-entropy alloys. *Curr. Opin. Solid State Mater. Sci.* **2022**, *26*, 101001. [[CrossRef](#)]
11. Kotomin, E.A.; Kuzovkov, V.N.; Popov, A.I. The kinetics of defect aggregation and metal colloid formation in ionic solids under irradiation. *Radiat. Eff. Defects Solids* **2001**, *155*, 113–125. [[CrossRef](#)]
12. Lu, Y.; Huang, H.; Gao, X.; Ren, C.; Gao, J.; Zhang, H.; Zhang, S.; Jin, Q.; Zhao, Y.; Lu, C. A promising new class of irradiation tolerant materials: Ti₂ZrHfV_{0.5}Mo_{0.2} high-entropy alloy. *J. Mater. Sci. Technol.* **2019**, *35*, 369–373. [[CrossRef](#)]
13. Kotomin, E.; Kuzovkov, V.; Popov, A.I.; Maier, J.; Vila, R. Anomalous kinetics of diffusion-controlled defect annealing in irradiated ionic solids. *J. Phys. Chem. A* **2018**, *122*, 28–32. [[CrossRef](#)] [[PubMed](#)]
14. Xia, S.; Gao, M.C.; Yang, T.; Liaw, P.K.; Zhang, Y. Phase stability and microstructures of high entropy alloys ion irradiated to high doses. *J. Nucl. Mater.* **2016**, *480*, 100–108. [[CrossRef](#)]
15. Yang, T.; Xia, S.; Guo, W.; Hu, R.; Poplawsky, J.D.; Sha, G.; Wang, Y. Effects of temperature on the irradiation responses of Al_{0.1}CoCrFeNi high entropy alloy. *Scr. Mater.* **2018**, *144*, 31–35. [[CrossRef](#)]
16. Yang, T.; Xia, S.; Liu, S.; Wang, C.; Liu, S.; Fang, Y.; Wang, Y. Precipitation behavior of Al × CoCrFeNi high entropy alloys under ion irradiation. *Sci. Rep.* **2016**, *6*, 32146. [[CrossRef](#)]
17. Cheng, Z.; Sun, J.; Gao, X.; Wang, Y.; Cui, J.; Wang, T.; Chang, H. Irradiation effects in high-entropy alloys and their applications. *J. Alloys Compd.* **2023**, *930*, 166768. [[CrossRef](#)]
18. Yang, L.; Ge, H.; Zhang, J.; Xiong, T.; Jin, Q.; Zhou, Y.; Ma, X. High He-ion irradiation resistance of CrMnFeCoNi high-entropy alloy revealed by comparison study with Ni and 304SS. *J. Mater. Sci. Technol.* **2019**, *35*, 300–305. [[CrossRef](#)]
19. Pu, G.; Lin, L.; Ang, R.; Zhang, K.; Liu, B.; Li, Q. Outstanding radiation tolerance and mechanical behavior in ultra-fine nanocrystalline Al_{1.5}CoCrFeNi high entropy alloy films under He ion irradiation. *Appl. Surf. Sci.* **2020**, *516*, 146129. [[CrossRef](#)]
20. Lv, Y.; Hu, R.; Yao, Z.; Chen, J.; Xu, D.; Liu, Y.; Fan, X. Cooling rate effect on microstructure and mechanical properties of Al_xCoCrFeNi high entropy alloys. *Mater. Des.* **2017**, *132*, 392–399. [[CrossRef](#)]
21. Cureton, W.F.; Tracy, C.L.; Lang, M. Review of swift heavy ion irradiation effects in CeO₂. *Quantum Beam Sci.* **2021**, *5*, 19. [[CrossRef](#)]
22. Skuratov, V.A.; Gun, K.J.; Stano, J.; Zagorski, D.L. In situ luminescence as monitor of radiation damage under swift heavy ion irradiation. *Nucl. Instrum. Methods Phys. Res. Sect. B Beam Interact. Mater. At.* **2006**, *245*, 194–200. [[CrossRef](#)]
23. Yablinsky, C.A.; Devanathan, R.; Pakarinen, J.; Gan, J.; Severin, D.; Trautmann, C.; Allen, T.R. Characterization of swift heavy ion irradiation damage in ceria. *J. Mater. Res.* **2015**, *30*, 1473–1484. [[CrossRef](#)]
24. Patra, P.; Shah, S.; Kedia, S.K.; Sulania, I.; Singh, M.J. Study on structural properties of swift heavy ion induced damage in Al₂O₃. *Radiat. Phys. Chem.* **2023**, *212*, 111128. [[CrossRef](#)]
25. Jia, Y.; Zhang, L.; Li, P.; Ma, X.; Xu, L.; Wu, S.; Wang, G. Microstructure and mechanical properties of Nb–Ti–V–Zr refractory medium-entropy alloys. *Front. Mater.* **2020**, *7*, 172. [[CrossRef](#)]
26. Rymzhanov, R.A.; Medvedev, N.; Volkov, A.E.; O'Connell, J.H.; Skuratov, V.A. Overlap of swift heavy ion tracks in Al₂O₃. *Nucl. Instrum. Methods Phys. Res. Sect. B Beam Interact. Mater. At.* **2018**, *435*, 121–125. [[CrossRef](#)]
27. Kamarou, A.; Wesch, W.; Wendler, E.; Undisz, A.; Rettenmayr, M. Swift heavy ion irradiation of InP: Thermal spike modeling of track formation. *Phys. Rev. B* **2006**, *73*, 184107. [[CrossRef](#)]
28. Zhumazhanova, A.; Mutali, A.; Ibrayeva, A.; Skuratov, V.; Dauletbekova, A.; Korneeva, E.; Zdorovets, M. Raman study of polycrystalline Si₃N₄ irradiated with swift heavy ions. *Crystals* **2021**, *11*, 1313. [[CrossRef](#)]
29. Wang, X.; Zhang, Y.; Liu, S.; Zhao, Z. Depth profiling by Raman spectroscopy of high-energy ion irradiated silicon carbide. *Nucl. Instrum. Methods Phys. Res. Sect. B Beam Interact. Mater. At.* **2014**, *319*, 55–61. [[CrossRef](#)]
30. Zhang, Z.; Armstrong, D.E.; Grant, P.S. The effects of irradiation on CrMnFeCoNi high-entropy alloy and its derivatives. *Prog. Mater. Sci.* **2022**, *123*, 100807. [[CrossRef](#)]
31. Xia, S.Q.; Wang, Z.; Yang, T.F.; Zhang, Y. Irradiation behavior in high entropy alloys. *J. Iron Steel Res. Int.* **2015**, *22*, 879–884. [[CrossRef](#)]

32. Kumar, N.K.; Li, C.; Leonard, K.J.; Bei, H.; Zinkle, S.J. Microstructural stability and mechanical behavior of FeNiMnCr high entropy alloy under ion irradiation. *Acta Mater.* **2016**, *113*, 230–244. [[CrossRef](#)]
33. Xu, Q.; Guan, H.Q.; Zhong, Z.H.; Huang, S.S.; Zhao, J.J. Irradiation resistance mechanism of the CoCrFeMnNi equiatomic high-entropy alloy. *Sci. Rep.* **2021**, *11*, 608. [[CrossRef](#)] [[PubMed](#)]
34. Koo, C.H.; Yu, T.H. Pack cementation coatings on Ti₃Al–Nb alloys to modify the high-temperature oxidation properties. *Surf. Coat. Technol.* **2000**, *126*, 171–180. [[CrossRef](#)]
35. Jiang, G.; Xu, D.; Liu, L.; Ding, X.; Kuang, W.; Wang, M. Oxidation of typical Zr–Nb alloy in high-temperature air under 700–900 °C. *Corros. Sci.* **2022**, *209*, 110701. [[CrossRef](#)]
36. Jiang, G.; Xu, D.; Yang, W.; Liu, L.; Zhi, Y.; Yang, J. High-temperature corrosion of Zr–Nb alloy for nuclear structural materials. *Prog. Nucl. Energy* **2022**, *154*, 104490. [[CrossRef](#)]
37. Małecką, J. Resistance to High-Temperature Oxidation of Ti–Al–Nb Alloys. *Materials* **2022**, *15*, 2137. [[CrossRef](#)] [[PubMed](#)]

Disclaimer/Publisher’s Note: The statements, opinions and data contained in all publications are solely those of the individual author(s) and contributor(s) and not of MDPI and/or the editor(s). MDPI and/or the editor(s) disclaim responsibility for any injury to people or property resulting from any ideas, methods, instructions or products referred to in the content.